PNAS RESEARCH ARTICLE | PSYCHOLOGICAL AND COGNITIVE SCIENCES

Dopaminergic mechanisms supporting hippocampal postencoding dynamics in humans

Claire J. Ciampa[a,1], Thomas M. Morin[a,b], Jourdan H. Parent[a], Alex Adornato[a], Jordyn L. Cowan[a], Katherine O'Malley[a], Rachel E. Marcus[a], Charlee Gordon[a], James D. Howard[a], Arielle Tambini[c], Cristina Cusin[d], Jacob Hooker[b], and Anne S. Berry[a,e]

Affiliations are included on p. 10.

Edited by Donald Pfaff, Rockefeller University, New York, NY; received September 22, 2025; accepted January 13, 2026

Deficits in dopamine function cause alterations in episodic memory. Converging evidence implicates dopamine in postencoding hippocampal mechanisms inferred to support long-term memory, though there is a lack of direct evidence in humans. We address this gap using pharmacological functional MRI (fMRI) and positron emission tomography (PET). Using a motivated reward encoding task on and off oral methylphenidate, we tested whether individual differences in baseline dopamine ([^{11}C]raclopride PET D2/3 receptor density) relate to drug-induced changes in hippocampal postencoding processes. Our study focused on healthy older adults, who are among those most vulnerable to memory decline and may benefit from pharmacologically enhancing dopamine. We found that methylphenidate administration was associated with improved memory performance relative to placebo for both high and low reward conditions. Older adults with high receptor density showed greater persistence of hippocampal multivoxel patterns into postencoding rest and stronger hippocampus-midbrain resting-state connectivity following encoding while on methylphenidate. These findings support the view that enhanced dopaminergic tone, verified through PET, directly modulates hippocampal postencoding dynamics in humans. Substantial variation in neurobiological effects was associated with individual differences in baseline dopamine function as older adults with high dopamine receptor density profiles showed preferential benefit of drug on hippocampal function, though these insights are qualified by null associations between memory performance and postencoding hippocampal activity. Individuals with lower dopamine receptor profiles showed preferential benefit of reward incentives suggesting altered sensitivity to extrinsic motivational factors depending on endogenous dopamine function.

dopamine | simultaneous PET/fMRI | reward memory | aging

Significance

There is substantial interest in the mechanisms by which dopamine modulates motivated memory and hippocampal activity, and particularly in processes that occur after encoding. Through a combination of molecular imaging and pharmacological manipulation, we provide the most direct demonstration to date linking the dopamine system with postencoding hippocampal dynamics in humans. Our findings provide evidence that the effects of a dopaminergic drug on hippocampal postencoding function are related to individual differences in baseline dopamine. This initial work suggests that pharmaceutical interventions are a viable strategy for modulating hippocampal processes, particularly in older adults, who are among those most vulnerable to hippocampal functional changes.

There is considerable variation in episodic memory ability across individuals, which can be linked to neurobiological factors including differences in endogenous dopamine function. Highly replicated findings indicate the density of dopamine receptors declines in older age (1, 2), and popular frameworks propose that receptor losses mediate reductions in memory performance across the lifespan (3). The beneficial impact of reward incentives on memory performance is maintained in aging (4), which, given dopamine's role in reward-motivated cognition, suggests that dopamine circuits can be successfully leveraged to enhance memory in older adults. Despite detailed mechanistic research on dopaminergic modulation of memory and neural activity in animal models (5–7), there is a need for basic research investigating how dopamine shapes memory-related functional brain imaging measures in humans to inform the development of future therapeutic interventions targeting the dopamine system.

Observations that reward-related memory enhancement is often minimal or absent immediately following encoding, but requires longer temporal delays (8–10) have underscored the importance of postencoding consolidation to long-term memory and suggest dopamine's involvement in these processes. Supporting this view, dopaminergic drugs often impact delayed, but not immediate measures of hippocampus-dependent cognition (11–13). Studies of postencoding mechanisms of synaptic plasticity directly implicate dopamine in the modulation of late long-term potentiation (14). Postencoding processes are also commonly studied by investigating the reappearance of encoding-related hippocampal activity patterns during later periods of rest, as observed in rodents and other nonhuman animals (15, 16). Critically, direct stimulation of dopaminergic inputs to the hippocampus during encoding has been shown to increase postencoding hippocampal replay and improve memory performance in rodent models (7).

Author contributions: C.J.C. and A.S.B. designed research; C.J.C., T.M.M., J.H.P., A.A., J.L.C., K.O., R.E.M., C.G., J.D.H., A.T., C.C., J.H., and A.S.B. performed research; C.J.C. analyzed data; and C.J.C. and A.S.B. wrote the paper.

Competing interest statement: J. Hooker is co-founder of and equity holder in Eikonizo Therapeutics and Sensorium Therapeutics, where he also serves as CEO. He is currently an advisor to Rocket Science Health, Human Health, Delix Therapeutics, and Psy Therapeutics.

This article is a PNAS Direct Submission.

[1]To whom correspondence may be addressed. Email: claireciampa@brandeis.edu.

This article contains supporting information online at https://www.pnas.org/lookup/suppl/doi:10.1073/pnas.2526799123/-/DCSupplemental.

Published February 5, 2026.

In human fMRI studies, previous research has leveraged pattern analyses to demonstrate that encoding activation patterns persist into postencoding rest (17). Gruber et al. (18) extended this work to show that persistence of multivoxel patterns can be modulated by monetary reward incentives and is accompanied by increased functional connectivity between dopaminergic midbrain nuclei and hippocampus, providing a link between postencoding fMRI measures and the dopaminergic reward system (19). In healthy young populations, pattern similarity between encoding and rest and increased resting-state functional connectivity (RSFC) are correlated with subsequent memory performance (17, 18, 20), indicating that the persistence of encoding-related processes into rest holds behavioral relevance and represents a meaningful measure for understanding the neural mechanisms supporting memory. There is currently a lack of direct evidence in humans that dopamine supports the persistence of task-related multivoxel patterns and functional connectivity, either by increasing dopamine pharmacologically or measuring endogenous dopamine function in vivo.

Evaluating baseline dopamine function is essential for interpreting the effects of dopamine drugs, which can vary widely depending on individual differences in baseline dopamine (21, 22). This finding was initially established in nonhuman animals (23, 24) and corroborated with human research demonstrating that effects of dopamine drugs on cognition and fMRI activation depend on genetic polymorphisms corresponding to individual differences in dopamine function (25). Positron emission tomography (PET) studies extended this work to show that baseline levels of dopamine synthesis capacity can predict the effects of a dopamine agonist on reversal learning (26). This research highlights the need to account for baseline dopamine when assessing the impacts of dopamine drugs on cognitive and neural processes. In particular, aging studies using pharmacological manipulations are often limited by lack of knowledge about the integrity of participants' dopamine systems.

The goal of the current study was to investigate how endogenous baseline dopamine function relates to drug and reward-induced changes in memory and postencoding hippocampal processes in healthy older adults. To test this, we collected fMRI scans on and off oral methylphenidate (20 mg), which increases synaptic dopamine by blocking dopamine reuptake (27, 28). During fMRI scanning, participants completed a reward-motivated encoding task followed by a resting-state scan to assess persistence of encoding-related processes into rest (Fig. 1*A*). Postencoding fMRI measures included 1) persistence of hippocampal activation, operationalized as the degree of correlation between hippocampal multivoxel patterns evoked during task encoding and those observed during each resting-state scan (17, 29), and 2) RSFC between the hippocampus and midbrain. While an extensive body of literature has demonstrated cortical pattern similarity during retrieval in both young and older adults (30, 31), spontaneous reinstatement of fMRI patterns during rest has been studied exclusively in young adults. It is currently unknown whether pattern reinstatement during rest occurs in older adults [but see (32) and (33) for studies demonstrating changes in functional connectivity in aging]. Critically, we assessed baseline D2/3 receptor density with [^{11}C]raclopride PET to investigate how individual differences in dopamine receptor profiles relate to reward and methylphenidate-induced changes in memory and postencoding dynamics. We hypothesized that both hippocampus-midbrain RSFC and multivoxel pattern similarity between encoding and rest would increase following the task, reflecting carryover or reactivation of encoding-related processes. Further, we predicted that individuals with the most intact dopamine systems would experience the strongest persistence of task-related processes.

Results

Memory Is Enhanced on Methylphenidate and for High Reward. Healthy older adult participants (n = 46) completed a reward-motivated encoding task during both placebo and drug scanning sessions (Fig. 1*B*). To-be-encoded images were shown on either a high reward background ($5 per remembered item) or a low reward background ($0.01 per remembered item). Encoding blocks were cued with a screen showing "High Reward" or "Low Reward" and reward amounts were overlaid on the background scenes. Memory was assessed 24 h later for 1) item recognition by showing participants an image and asking if they had viewed the image during scanning, and 2) object-context associative memory in which participants were asked to match images with the correct background context (high or low reward).

Item recognition results showed expected effects of drug and reward. Specifically, a Drug*Reward linear mixed effects model (LME with a random intercept) predicting item memory (hit rate – false alarm rate) demonstrated methylphenidate enhanced memory performance relative to placebo (main effect of Drug: t = 2.88, $P = 0.005$, $f^2 = 0.07$; Fig. 1*C* and Table 1). This finding is consistent with work in young adults demonstrating that methylphenidate can improve long-term memory performance (34). Monetary incentives also enhanced memory such that participants recognized more items viewed within high reward contexts compared with items viewed within low reward contexts (main effect of Reward: t = 3.98, $P = 0.0001$, $f^2 = 0.14$). This aligns with previous work demonstrating intact effects of reward on memory in older adults (35, 36). We did not find evidence that drug altered the impact of reward on memory (Drug*Reward interaction: t = –0.47, $P = 0.64$, $f^2 = 0.002$).

As a large proportion of participants performed below chance level for object-context memory for one or more task conditions (>22% below chance across all drug and reward conditions), we focused our analyses on item memory. Results for the Drug*Reward interaction on object-context memory are reported in *SI Appendix* and presented in *SI Appendix*, Fig. S1.

[^{11}C]raclopride BP_{ND} Decreases on Drug. [^{11}C]raclopride is a commonly used dopamine PET tracer, particularly in studies on aging (2, 37, 38), and provides a measure of D2/3 receptor density. [^{11}C]raclopride binds competitively with dopamine to D2/3 receptors, and enhancement of synaptic dopamine causes decreases in [^{11}C]raclopride signal (28, 39). Consistent with work in young adults (40), we demonstrated a significant decrease in [^{11}C]raclopride nondisplaceable binding potential (BP_{ND}, abbreviated D2DR) from placebo to drug in dorsal caudate (DCA) in our sample of healthy older adults (t = –4.96, $P = 0.0001$, $f^2 = 1.54$; Fig. 1*D*). Due to a low number of participants with both placebo and drug [^{11}C]raclopride scans (n = 17), we focus subsequent analyses on the larger sample of participants with baseline (placebo) [^{11}C]raclopride and fMRI/behavior across both placebo and drug conditions (n = 31). These displacement findings, however, provide critical proof of concept that methylphenidate caused measurable and significant increases in dopamine tone in our older adult population. We chose to analyze D2DR in DCA as this region has previously been implicated in hippocampus-related memory function (37). In older adults, higher D2/3 receptor density was directly related to better episodic memory and hippocampal RSFC (37).

Multivoxel Hippocampal Patterns Carry Over Into Rest. Hippocampal activation patterns carry over into rest in young adults (17), but it is currently unknown whether multivoxel

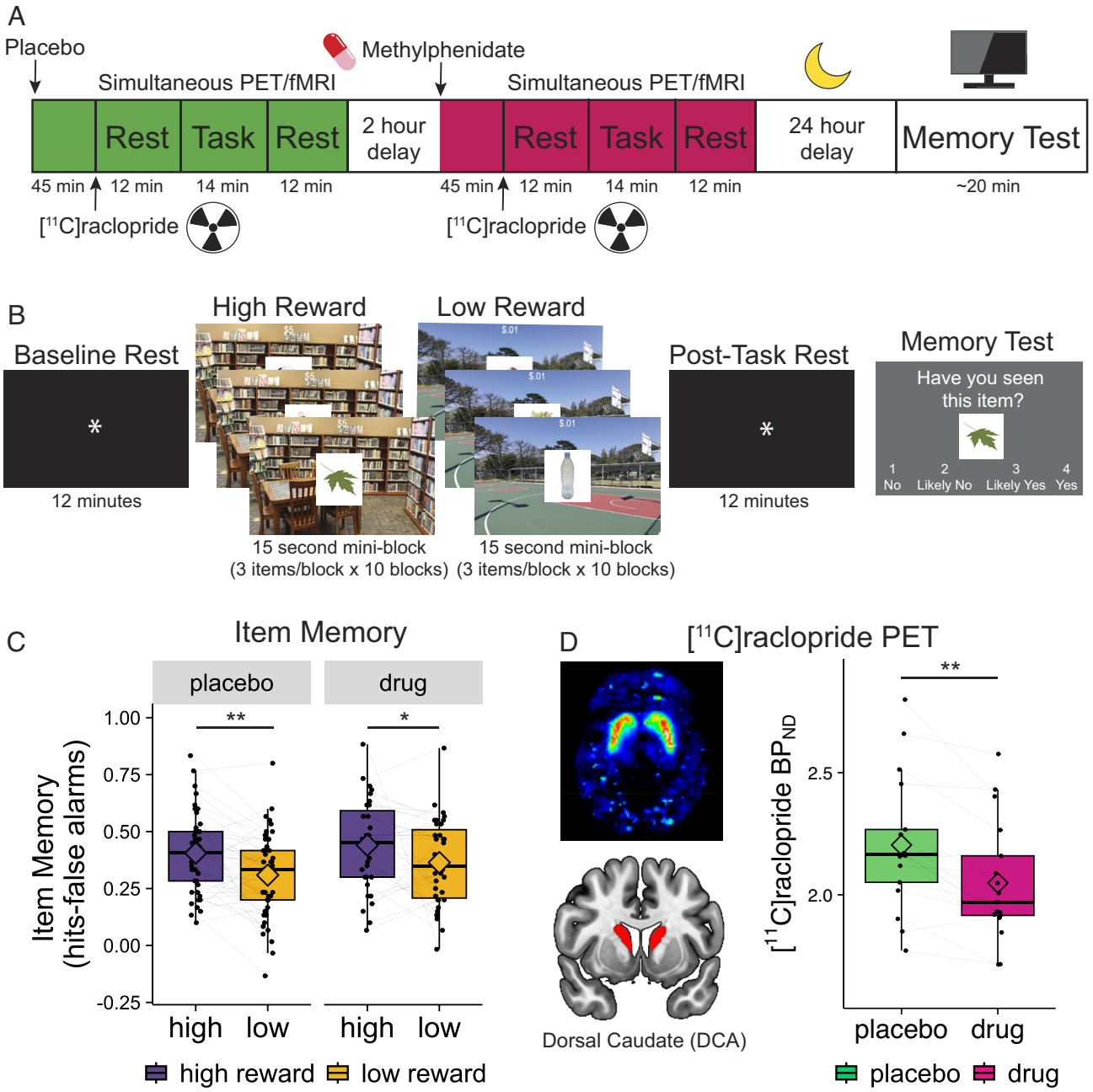

Fig. 1. Study design, behavioral results, and effect of drug on [^{11}C]raclopride. (*A*) Participants completed two fMRI scans, the first on placebo and the second on methylphenidate. Each scan included a reward task and resting-state fMRI scans immediately before and after the task. [^{11}C]raclopride dopamine PET was collected during each scanning session. (*B*) During each scanning session, participants encoded images overlaid on two different backgrounds associated with high ($5) and low reward ($0.01). Item recognition memory was assessed during a surprise memory test 24 h after scanning. (*C*) Effects of drug and reward on item recognition memory (hit rate − false alarm rate). Placebo n = 46, drug n = 35. (*D*) An example participant's native space [^{11}C]raclopride PET scan (*Top Left*). [^{11}C]raclopride was measured in dorsal caudate (DCA), displayed in red (*Bottom Left*). DCA [^{11}C]raclopride nondisplaceable binding potential (BP_{ND}, abbreviated as D2DR) decreased on drug (pink) relative to placebo (green). Placebo n = 17, drug n = 17. *P < 0.01, **P < 0.001.

patterns persist into rest in older adults. To investigate fMRI pattern similarity between encoding and rest, we used a previously developed method that involves correlating pairs of time series for every voxel in the hippocampus to create multivoxel correlation structure (MVCS) matrices that reflect voxel coactivation patterns (17). We computed these matrices separately for high and low reward encoding, pretask rest, and posttask rest for each participant. A representative participant's MVCS matrices are shown in Fig. 2*A*. We then correlated the encoding MVCS matrices with each rest matrix to obtain pre- and posttask similarity values (Fisher z-transformed Pearson's correlation coefficient). If task-related activation patterns carry over into rest, similarity between encoding and rest should be higher for posttask relative to baseline pretask rest, indicating that patterns of encoding-related activation established during the task are reinstated following the task. We tested this hypothesis at the group level using a Drug*Reward*Stage interaction predicting the Fisher z-transformed correlations between MVCSs. We found that similarity between encoding and rest increased posttask relative to pretask (main effect of Stage: t = 3.22, P = 0.001, f^2 = 0.05; Fig. 2*B* and Table 2*A*), suggesting that encoding-related activation patterns persist beyond the task. Although there was no Stage*Drug interaction (t = −0.46, P = 0.65, f^2 = 0.001), for completeness, we note that the main

Table 1. Drug*Reward interaction on item memory using a linear mixed effects (LME) model

Variable	Unstandardized Coef.	SE	t-value	*P*-value	95% CI (Lower)	95% CI (Upper)
Item memory ~ Drug*Reward + Age + Sex						
(Intercept)	0.23	0.31	0.75	0.46	−0.40	0.86
Drug	0.03	0.01	2.88	0.01	0.01	0.06
Reward	0.04	0.01	3.98	<0.01	0.02	0.07
Age	0.00	0.00	0.24	0.81	−0.01	0.01
Sex	0.06	0.04	1.30	0.20	−0.03	0.14
Drug*Reward	−0.01	0.01	−0.47	0.64	−0.03	0.02

The dependent variable is adjusted hit rate (hit rate − false alarm rate). Covariates include age and sex.

effect of Stage appears to be driven by the placebo scan for both high reward (t = 2.53, $P = 0.02$, $f^2 = 0.18$) and low reward (t = 2.44, $P = 0.02$, $f^2 = 0.16$) and was not observed at the group level on drug for either high reward (t = 0.79, $P = 0.44$, $f^2 = 0.02$) or low reward (t = 1.48, $P = 0.15$, $f^2 = 0.08$), which may be due to greater individual variation in pattern similarity on drug. There was also no main effect of Reward or interactions with Reward ($P > 0.23$), suggesting that reward does not modulate pattern similarity. Together, these results demonstrate that persistence of activation patterns into rest can be observed in older adults, but that modulation of these effects by drug and reward is not consistent on a group level.

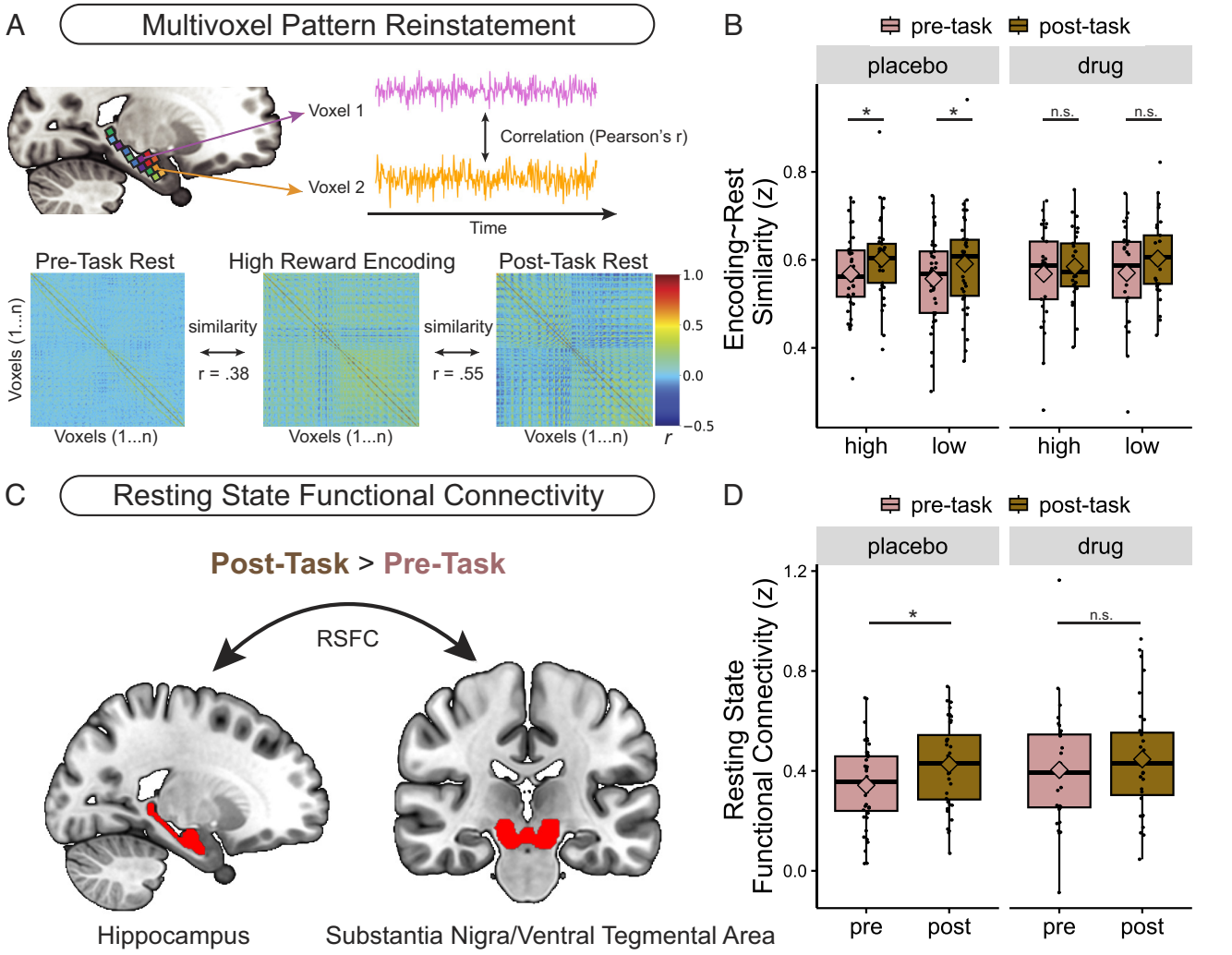

Fig. 2. Multivoxel pattern reinstatement and resting-state functional connectivity (RSFC). (*A*) Time series were extracted from each hippocampal voxel and correlated with the time series for every other voxel in the hippocampus to create multivoxel correlation structures (MVCSs), which are shown for an example participant for pretask rest, high reward encoding, and posttask rest. Colors in the matrices represent correlation values between pairs of voxel time series. (*B*) Group-level reinstatement analyses examining the difference in Fisher z-transformed encoding ~ rest correlations for posttask rest (brown) relative to pretask rest (pink). Panels split analyses by placebo and drug scanning sessions, with high and low reward on the x-axis. Placebo n = 37, drug n = 29. (*C*) Schematic showing hippocampus–SN/VTA RSFC. (*D*) Group-level hippocampus–SN/VTA RSFC analyses testing for differences between pretask and posttask connectivity, split by placebo and drug sessions. Placebo n = 40, drug n = 31. *$P < 0.05$

Table 2. (*A*) Drug*Reward*Stage interaction on pattern similarity using a linear mixed effects (LME) model; (*B*) Drug*Stage interaction LME model on resting-state functional connectivity (RSFC)

Variable	Unstandardized Coef.	SE	*t*-value	*P*-value	95% CI (Lower)	95% CI (Upper)
(*A*) Pattern similarity ~ Drug*Reward*Stage + Age + Sex						
(Intercept)	0.23	0.15	1.56	0.13	−0.07	0.54
Drug	−0.00	0.01	−0.11	0.91	−0.01	0.01
Reward	0.00	0.01	0.01	0.99	−0.01	0.01
Stage	0.01	0.01	3.22	<0.01	0.01	0.02
Age	0.01	0.00	2.93	0.01	0.00	0.01
Sex	−0.05	0.02	−2.27	0.03	−0.09	−0.01
Drug*Reward	−0.01	0.01	−1.19	0.23	−0.01	0.00
Drug*Stage	−0.00	0.01	−0.46	0.65	−0.01	0.01
Reward*Stage	−0.00	0.01	−0.45	0.65	−0.01	0.01
Drug*Reward*Stage	−0.00	0.01	−0.48	0.63	−0.01	0.01
(*B*) Resting-state functional connectivity (RSFC) ~ Drug*Stage + Age + Sex						
(Intercept)	1.20	0.32	3.71	<0.01	0.54	1.85
Drug	0.02	0.01	1.40	0.16	−0.01	0.04
Stage	0.03	0.01	2.49	0.01	0.01	0.06
Age	−0.01	0.01	−2.39	0.02	−0.02	−0.00
Sex	−0.03	0.04	−0.58	0.57	−0.12	0.07
Drug*Stage	−0.01	0.01	−0.80	0.42	−0.04	0.01

Models adjust for age and sex as covariates

Hippocampus–SN/VTA RSFC Increases After Encoding. Midbrain dopamine-producing nuclei (substantia nigra and ventral tegmental area, SN/VTA) have previously been linked with hippocampus-related reward-motivated memory processes (18, 41). If our reward-motivated memory task influences hippocampal–SN/VTA interactions, we would expect RSFC between these regions to increase following the task relative to baseline rest (Fig. 2*C*). We tested this using a Drug*Stage interaction analysis predicting RSFC (Fisher z-transformed Pearson's correlation between average time series for the hippocampus and SN/VTA). Similar to the multivoxel pattern analysis, RSFC was stronger during posttask rest relative to pretask rest, in line with proposals that communication between these regions is enhanced following the task (main effect of Stage: t = 2.49, P = 0.01, f^2 = 0.06; Fig. 2*D* and Table 2*B*). There was no main effect of Drug and no Stage*Drug interaction (P > 0.16). However, the difference between pre- and posttask rest was limited to the placebo scan (t = 3.24, P = 0.002, f^2 = 0.27) and was not observed on drug (t = 0.87, P = 0.39, f^2 = 0.02). These findings mirror the pattern similarity results and indicate that communication between the hippocampus and midbrain increases immediately after encoding.

Drug Effects on Postencoding Neural Dynamics Relate to Baseline D2DR. A major goal of our study was to investigate whether endogenous baseline dopamine, measured with [^{11}C] raclopride PET, could predict drug-related changes in hippocampal postencoding processes. To examine relationships between D2DR and pattern similarity, we tested a Drug*Reward*D2DR interaction predicting pattern similarity between encoding and rest (posttask – pretask; Fig. 3*A* and Table 3*A*). Higher D2DR related to higher pattern similarity for both high and low reward on drug but not placebo (Drug*D2DR interaction: t = 4.80, P = 0.00001, f^2 = 0.39). This finding is consistent with studies showing that incorporating baseline measures of dopamine is necessary for interpreting drug effects (21). In a separate model, we also tested whether D2DR related to the difference in pattern similarity from placebo to drug (drug-placebo) but found no significant effect of D2DR (main effect of D2DR: t = 1.60, P = 0.14, f^2 = 0.20; Fig. 3*B*).

We next conducted parallel analyses testing for relationships between hippocampus–SN/VTA RSFC and D2DR. Consistent with the pattern similarity analysis, higher D2DR related to stronger RSFC (post-pre) on drug but not placebo (Drug*D2DR interaction: t = 3.20, P = 0.004, f^2 = 0.44; Fig. 3*C* and Table 3*B*). Additionally, higher D2DR related to greater difference in RSFC from placebo to drug (drug-placebo; t = 2.43, P = 0.03, f^2 = 0.67; Fig. 3*D*).

Reward Improves Memory for Individuals With Low D2DR. After establishing that D2DR predicts change in hippocampal postencoding measures, we conducted parallel analyses investigating whether D2DR also predicts change in memory performance. We first tested a Drug*Reward*D2DR interaction predicting item memory (hit rate – false alarm rate). There was no significant three-way interaction predicting item memory (t = 0.76, P = 0.45, f^2 = 0.009). There was a significant main effect of Reward (t = 2.83, P = 0.006, f^2 = 0.12), which was qualified by a significant Reward*D2DR interaction (t = –2.48, P = 0.02, f^2 = 0.09; Fig. 4 and Table 3*C*). There were no other significant main effects or interactions (P > 0.15). Post hoc regressions probing the Reward*D2DR interaction revealed that lower D2DR related to better memory for high reward collapsing across drug conditions (t = –2.64, P = 0.01, f^2 = 0.28) whereas there was no relationship between D2DR and low reward collapsing across drug conditions (t = –0.55, P = 0.59, f^2 = 0.02). This finding suggests that individuals with lower D2/3 receptor density are most sensitive to reward incentives.

Hippocampal Reinstatement and Hippocampus–SN/VTA RSFC Do Not Relate to Memory Performance. While reinstatement and hippocampus–SN/VTA connectivity have been linked with memory performance in young adults (18), we did not find evidence that either of these fMRI measures relate to memory in

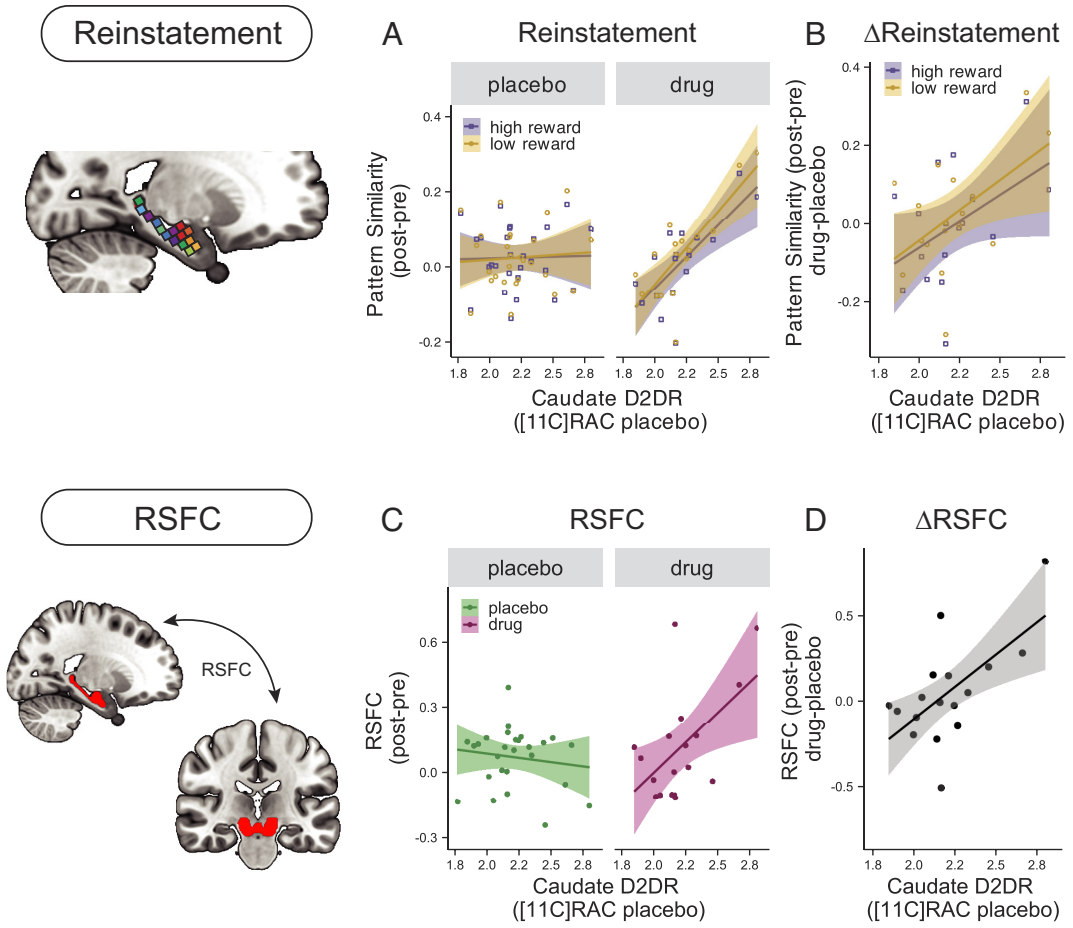

Fig. 3. Associations between baseline DCA D2DR and fMRI postencoding measures. (*A*) Relationship between baseline (placebo) D2DR and hippocampal reinstatement (pattern similarity, post-pre) split by high reward (purple) and low reward (gold) for placebo and drug scans. Placebo n = 27, drug n = 17. (*B*) Relationship between D2DR and difference in reinstatement from placebo to drug (drug-placebo), n = 17. (*C*) Relationship between caudate D2DR and hippocampus–SN/VTA RSFC (post-pre) for placebo and drug. Placebo n = 27, drug n = 18. (*D*) Relationship between D2DR and drug-placebo difference in RSFC (post-pre), n = 18.

our sample of older adults. Results for these analyses are reported in *SI Appendix* and displayed in *SI Appendix*, Fig. S2.

Discussion

This study advances our understanding of the mechanisms underlying human episodic memory and hippocampal processes in the following ways. First, by combining pharmacology and assessment of baseline dopamine function, we directly implicate dopamine in the modulation of postencoding fMRI dynamics. Second, we demonstrate that baseline dopamine function can be used to forecast the degree to which an individual may benefit from reward incentives versus acute pharmacological treatment (Fig. 5). Relevant to human aging, we replicate past research demonstrating that monetary reward enhances memory in older adults. We additionally demonstrate that encoding-related hippocampal pattern activity patterns persist during later periods of rest in healthy aging. Further, we verify that methylphenidate increases the availability of synaptic dopamine as measured by PET and improves episodic memory, which has not, to our knowledge, been previously established in older adult humans. Together, these findings support the viability of targets for enhancing human memory and provide direct mechanistic insight into how endogenous dopamine function shapes brain activity and behavior.

We complement and extend a growing body of research on postencoding dynamics in humans by providing evidence supporting the view that these fMRI signatures are modulated by dopamine. Specifically, we demonstrate that the pharmacological responsivity of two established fMRI measures, posttask pattern similarity and hippocampus–SN/VTA connectivity, is directly related to individual differences in dopamine function as measured with PET. We did not find that methylphenidate significantly increased pattern similarity or connectivity on a group level but instead found that these fMRI signatures were directly related to D2/3 receptor density profiles. These findings align with prior work in young adults demonstrating that baseline dopamine predicts effects of drugs (26) and suggest that older adults with the most well-maintained dopamine systems may display the largest boosts in hippocampal function from pharmaceutical enhancements in dopamine.

In contrast to classic inverted U-shaped effects whereby individuals with deficient dopamine function benefit most from pharmacological augmentation (21), we found that drug did not strengthen postencoding fMRI signatures in those older adults with lowest D2DR profiles. These findings suggest that sustained increases in dopamine availability through pharmacological enhancement overwhelms or "overdoses" the system in individuals with very low receptor density. Additional research using lower drug doses would be needed to test this hypothesis for low receptor

Table 3. (*A*) Relationship between baseline dorsal caudate (DCA) D2DR and reinstatement (pattern similarity, post-pre); (*B*) Relationship between baseline DCA D2DR and RSFC; (*C*) Relationship between baseline DCA D2DR and item memory (hit rate − false alarm rate)

Variable	Unstandardized Coef.	SE	*t*-value	*P*-value	95% CI (Lower)	95% CI (Upper)
(*A*) Pattern similarity (post-pre) ~ D2DR*Drug*Reward + Age + Sex						
(Intercept)	−0.77	0.26	−2.96	0.01	−1.31	−0.23
Caudate D2DR	0.21	0.06	3.76	<0.01	0.09	0.33
Drug	−0.36	0.08	−4.75	<0.01	−0.51	−0.21
Reward	0.03	0.07	0.48	0.63	−0.11	0.18
Age	0.00	0.00	1.51	0.15	−0.00	0.01
Sex	0.02	0.03	0.90	0.38	−0.03	0.08
Caudate D2DR*Drug	0.16	0.03	4.80	<0.01	0.10	0.23
Caudate D2DR*Reward	−0.02	0.03	−0.56	0.58	−0.08	0.05
Drug*Reward	0.02	0.07	0.24	0.81	−0.13	0.16
Caudate D2DR*Drug*Reward	−0.01	0.03	−0.32	0.75	−0.07	0.06
(*B*) RSFC (post-pre) ~ D2DR*Drug + Age + Sex						
(Intercept)	−0.64	0.64	−1.00	0.33	−1.94	0.67
Caudate D2DR	0.28	0.13	2.13	0.04	0.01	0.56
Drug	−0.71	0.23	−3.08	0.01	−1.18	−0.23
Age	0.00	0.01	0.10	0.92	−0.01	0.01
Sex	0.03	0.06	0.53	0.60	−0.10	0.17
Caudate D2DR*Drug	0.33	0.10	3.20	<0.01	0.12	0.54
(*C*) Item Memory ~ D2DR*Drug*Reward + Age + Sex						
(Intercept)	0.87	0.59	1.48	0.15	−0.34	2.07
D2DR	−0.19	0.13	−1.50	0.15	−0.45	0.07
Drug	−0.06	0.11	−0.56	0.58	−0.27	0.15
Reward	0.28	0.10	2.83	0.01	0.08	0.48
Age	−0.00	0.01	−0.12	0.90	−0.01	0.01
Sex	0.02	0.06	0.26	0.80	−0.11	0.14
D2DR*Drug	0.05	0.05	0.97	0.34	−0.05	0.14
D2DR*Reward	−0.11	0.04	−2.48	0.02	−0.20	−0.02
Drug*Reward	−0.09	0.10	−0.86	0.39	−0.28	0.11
D2DR*Drug*Reward	0.03	0.04	0.76	0.45	−0.06	0.12

Models are LME interaction models adjusting for age and sex.

participants. However, it is important to note that these low receptor individuals showed the greatest impact of reward incentives on memory performance. These findings are broadly consistent with previous work in young adults, which established greater behavioral gains for rewarded Stroop trials in individuals with low caudate dopamine synthesis capacity rather than high dopamine synthesis capacity (42). Further, individuals carrying genetic polymorphisms associated with lower striatal D2 receptor density have been shown to exhibit greater reward sensitivity (43). Together these findings speak to the potential of motivation-based interventions to improve cognitive performance for low-dopamine individuals. Work using cognitive neurostimulation and instructed neurofeedback has demonstrated that instructed motivation can activate the dopamine system and improve long-term memory performance (44, 45). Though lower pharmacological dosing may prove effective, strategies to heighten motivation and transiently engage the dopamine system may be attractive intervention approaches for older adults with lower dopamine function.

Our study provides evidence of postencoding increases in hippocampal pattern similarity in older adults and extends previous literature investigating postencoding functional connectivity increases in aging (32, 33). This initial demonstration that postencoding effects are observed in aging is noteworthy in light of a related body of work, which has demonstrated age-related dysregulation of neural representations. Generally, aging is accompanied by dedifferentiation of brain networks (46), and relevant to memory processes, a decline in the quality of perceptual representations (47) and reductions in multivoxel similarity between encoding and retrieval hippocampal fMRI patterns (48). There are also alterations in the type of information that is successfully encoded, with age-related shifts toward gist-based (49), or categorical representations (47). The current study is limited by lack of a young adult comparison group, and it will be important for future studies to probe age-group differences in the type of information that is carried over from encoding to rest, and whether item-specific representations or perceptual features can be decoded in older brains.

While we found evidence that hippocampal patterns persisted into postencoding rest, this postencoding effect appeared to be relatively decoupled from later memory performance. Though we limit our interpretation of null results, it is notable that reward incentives significantly enhanced memory but did not modify the degree of hippocampal pattern similarity despite findings demonstrating reward-related increases in reinstatement in young adults (18). Future studies may investigate whether and how aging impacts reward's modulating effects on multivoxel patterns using high-resolution fMRI. Such studies would support analyses specifically targeting the anterior hippocampus, which may be more

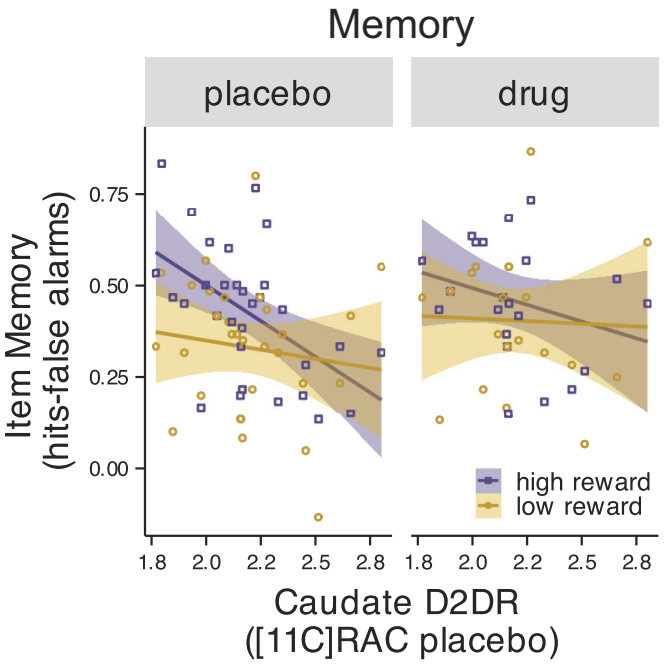

Fig. 4. Associations between DCA D2DR and memory. Relationship between D2DR (placebo) and item memory (hit rate − false alarm rate) for placebo and drug. Placebo n = 31, drug n = 21. High reward memory is shown in purple, and low reward memory is shown in gold.

sensitive to reward-motivated memory effects (19). Future work is also needed to investigate memory tasks without an explicit reward component to define the extent to which linkages among endogenous dopamine function, dopamine augmentation, and hippocampal signatures are observed generally following encoding or rely on the promise of monetary reward. Independent of reward, we did not detect significant associations between memory performance and either postencoding pattern similarity or functional connectivity increases in our current older adult sample. Though there is strong evidence that postencoding fMRI signatures are related to better subsequent memory performance (17, 18, 20), other work has found no relationship between pattern similarity and cognition (50). Other studies suggest that pattern similarity may relate to information that is forgotten over time rather than remembered (51) and that pattern similarity prioritizes weakly encoded information (52). These studies point to a nuanced role for persistence of activation patterns in memory processes, which may also interact with age. Memory performance in our participants may have depended more heavily on later consolidation processes, such as those that occur during sleep, which were not examined in this study.

This study is limited by our inability to account for other age-related factors impacting hippocampal function and episodic memory, most notably the accumulation of age and Alzheimer's disease (AD)-related tau pathology. While there are active lines of research investigating interactions among tau pathology, sleep, and episodic memory in aging (53) there is a lack of AD-relevant research incorporating multivariate fMRI approaches for examining pathology's impact on encoding and postencoding dynamics. The current study relied on PET imaging to assess endogenous dopamine function and was thus limited in sample size. Due to the small sample size, we were limited in our ability to detect interaction effects, and further work with larger samples is needed to replicate our findings. Recent work has explored novel techniques for investigating dopamine function in humans, including hemodynamic latency in the striatum and neuromelanin-sensitive structural scanning of the substantia nigra (54, 55). Further development of these techniques will provide less invasive and more accessible alternatives to PET scanning and promise to support better integration of findings across fields of cognitive and

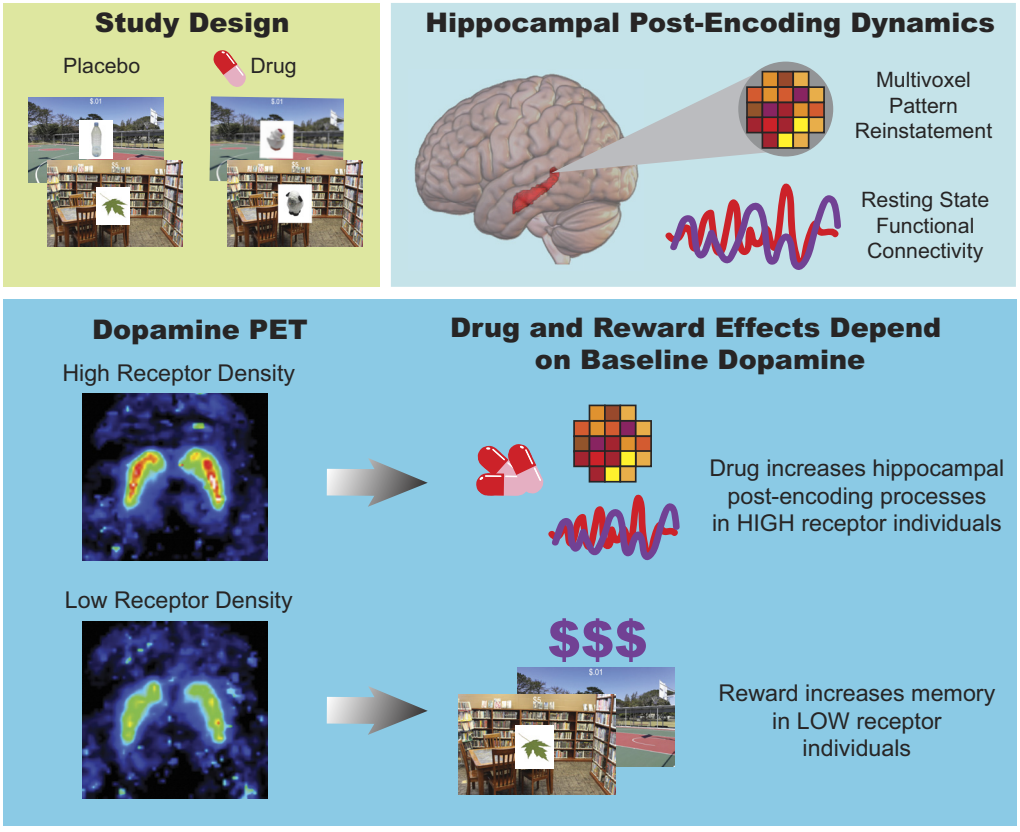

Fig. 5. Graphical summary. Participants were scanned on and off drug (methylphenidate) while completing a reward-motivated encoding task (*Top Left*). Postencoding hippocampal dynamics included multivoxel pattern similarity between encoding and rest and RSFC between the hippocampus and dopaminergic midbrain regions (*Top Right*). Individuals with the highest caudate D2/3 dopamine receptor density, measured with [^{11}C]raclopride PET scanning, exhibited the greatest postencoding drug-related increases in hippocampal processes, while individuals with lower D2/3 receptor density demonstrated the greatest reward-related increases in memory performance (*Bottom* panel).

systems-level neuroscience. The drug scan was always completed second due to the amount of time methylphenidate takes to metabolize. This raises the possibility that the drug effects observed in this study were confounded by order effects. While we do not anticipate strong practice effects due to the passive encoding nature of the task and prior practice before the first scanning session, previous work has shown that order effects moderate the impact of dopaminergic drugs (56). This points to the value of future work using crossover designs.

In summary, this study sheds light on the role of dopamine in modulating postencoding fMRI dynamics in humans and underscores the necessity for understanding individual differences in endogenous dopamine function for interpreting responses to reward incentives and pharmacological treatment.

Materials and Methods

Participants. Our sample included 46 healthy older adult participants (60 to 82 y old, mean age = 69.24, 52% female). Details on participant attrition and exclusions are reported in *SI Appendix* under Detailed Methods and are displayed in *SI Appendix*, Fig. S3. Participants were recruited from the greater Boston area as part of the Brandeis Aging Brain Study and underwent neuropsychological testing to establish that they are cognitively normal. Inclusion criteria are at least 12 years of education, a Mini Mental State Exam (MMSE) score greater than 26, and a Geriatric Depression Scale (GDS) score less than 13. Participants did not have a history of neurological, psychological, or systemic medical illness affecting cognition (such as a brain tumor, late-stage cancer, hepatic failure, chronic severe pulmonary disease, or large cortical infarcts). Additionally, participants were not taking stimulant medications and did not have MRI contraindications. The Brandeis University Human Research Protection Program and the Massachusetts General Brigham (MGB) Partners Human Research Protection Program approved this study. Participants provided written informed consent and received monetary compensation for their participation.

Reward Memory Encoding Task. The reward motivated memory task was adapted from Gruber et al. (18) and was carried out during both placebo and drug scanning sessions. Of the 46 participants in our sample, 35 had drug behavioral data. During placebo and drug scans, participants completed block-design fMRI runs in which they were asked to encode the objects that appeared on the screen. Blocks were 15 s each (3 images/block, 10 blocks/run) and alternated between "high reward" encoding conditions ($5 for each remembered item) and "low reward" encoding conditions ($0.01 for each remembered item). Stimuli appeared in either high reward or low reward "contexts" (background scenes). Reward blocks were cued with a slide showing the words "High Reward" or "Low Reward" before the start of each block. Text showing the reward amount ($5 or $0.01) appeared on the screen overlaid on the background images. Before beginning the scanning sessions, participants were reminded of which background was associated with which reward condition and were asked to verbally confirm their knowledge of the reward background scenes. Between each encoding block was an inter-block period in which participants pressed right or left buttons in response to arrows presented on the screen. This condition was designed to prevent continued rehearsal/encoding during baseline measurements. Participants completed a short memory test immediately after both runs of the encoding task, during which they were shown 8 items and asked to indicate whether they had viewed the items during the encoding task. The purpose of this immediate memory test was to prevent continued rehearsal during the posttask resting-state scan, as has been done in past work (19). Data from this immediate memory test were not analyzed. Twenty-four hours after the second scanning session, participants were given a surprise memory test (outside of the scanner) to assess memory for 1) item recognition and 2) item–context associations. During the surprise memory test, they viewed 60 old items previously seen in the scanner (30 high reward items and 30 low reward items) and 60 new items. To assess item memory, they were first shown an image and asked to rate their confidence in whether the item was old (1 = New, 2 = Likely New, 3 = Likely Old, 4 = Old). If they selected Old or Likely Old, they were then asked to match the image with the correct background on which the image had appeared (context memory). For behavioral and fMRI analyses, we collapsed across item memory confidence ratings such that items rated "3" and "4" were both considered "Old" and items rated "1" and "2" were both considered "New." For both item and context memory, the primary measure of interest was adjusted hit rate (hit rate − false alarm rate), where hit rate was defined as the number of correctly identified old items divided by the number of total old items, and false alarm rate was the number of new (lure) items incorrectly identified as old items divided by the total number of lures. To limit potential practice effects, participants practiced the task on a computer outside of the scanner before the first scanning session. Participants viewed different items for placebo and drug scans, and item order was randomized across participants. Approximately half of participants viewed a library background scene as high reward and a basketball court as low reward, while the other half of participants viewed library as low reward and basketball court as high reward.

Effects of drug and reward on adjusted hit rate were assessed using a LME with a random intercept and a fixed slope [hit rate − false alarm rate ~ drug*reward + age + sex + (1|subject)].

fMRI Data Acquisition and Preprocessing. There were four blood-oxygen-level-dependent (BOLD) fMRI scans under placebo conditions, and four BOLD scans under methylphenidate conditions: a pre-encoding 12-min resting-state scan followed by two 7-min reward-encoding task runs (block design) and finally a postencoding 12-min resting-state scan. Forty participants had usable resting-state placebo fMRI data, and 31 participants had usable resting-state drug fMRI data. Of these participants, 37 had usable task encoding placebo fMRI data and 29 had usable task encoding drug fMRI data. During each resting-state scan, participants were asked to remain still and to look at a white asterisk in the middle of a black screen. Data were collected on a custom-built joint PET/MR 3 T Siemens TIM Trio with a BrainPET insert using an 8-channel head coil (57). Functional MRI (fMRI) scans were collected using a T2*-weighted gradient-echo planar pulse (EPI) sequence (TR = 2,000 ms; TE = 30 ms; flip angle = 90°; FOV = 200 mm; 37 slices, oriented AC-PC; voxel size = 3.1 × 3.1 × 3.0 mm). A T1-weighted structural scan was acquired for preprocessing purposes.

Preprocessing was performed in fMRIPrep (v22.0.2), including slice timing correction, head motion and confound estimation, EPI to T1 registration, and resampling to MNI152 template space. Details on the fMRIPrep pipeline are reported in Supplemental Information under the section fMRI Preprocessing with fMRIPrep. Analysis and Visualization of Functional Neuroimages (AFNI) software (v7.64) was used to further process the MNI space images. AFNI processing included denoising using aCompCor (first six components from the combined white matter/CSF mask generated by fMRIPrep) and a high-pass filter of 0.008 Hz (128 s). Data were smoothed to a 2 mm full width half maximum (FWHM) kernel. Frames containing motion greater than 0.5 mm were scrubbed and any scans in which more than 20% of frames were scrubbed were excluded from analyses. Motion correction was performed by regressing out the six head motion parameters (three translations and three rotations) along with their first-level derivatives from the time series data. 0 to 3rd order polynomial trends were also regressed out to adjust for linear and polynomial trends. After regressing nuisance variables out of the time series data, individual voxels in the hippocampus were removed if they showed excessive noise (SD of all time points >5 SD from the mean temporal SD of all hippocampal voxels) or if they showed potential signal dropout (mean signal <2 SD below mean signal of all hippocampal voxels), as done previously (17).

Defining Regions of Interest (ROIs). A bilateral hippocampal ROI was anatomically defined in MNI space using FreeSurfer (v6.0.0). DCA was manually drawn in ITK SNAP software (v4.0.1) on each participant's native space T1 scan using a previously developed protocol (58) for use in PET analyses. For participants with both drug and placebo T1 scans, the T1 scans were first merged using FreeSurfer's "recon-all -base" command to create an unbiased merged template (59). Before drawing ROIs, T1 scans were realigned to the anterior–posterior commissure (AC-PC) line. DCA was drawn anterior to the AC for both left and right hemispheres. For participants with both placebo and drug scans, DCA was drawn on the merged scan and then coregistered to the AC-PC realigned native space placebo and drug T1 scans. The midbrain ROI combined substantia nigra (SN) and ventral tegmental area (VTA) and was defined using a probabilistic atlas (60) and thresholded such that voxels with a 50% or greater probability of being in the SN/VTA were included in the ROI.

fMRI Encoding-Rest Pattern Similarity. We tested for reinstatement between encoding and rest using an analysis adapted from rodent electrophysiology studies (17). Similar to previous work (17, 29, 50), we calculated MVCSs by correlating denoised hippocampal time series for each voxel with the time series for every other voxel in the hippocampus, which results in an $n \times n$ matrix of Fisher z-transformed Pearson's correlation values, where n is the number of voxels in the hippocampal ROI. This matrix represents the pattern of coactivation across different voxels and provides a measure of multivoxel BOLD patterns. We created four separate MVCS matrices for each participant: 1) high reward encoding (concatenating across blocks and runs), 2) low reward encoding (concatenating across blocks and runs), 3) pretask rest, and 4) posttask rest. As the matrices are symmetric about the diagonal, only the upper half of each matrix was analyzed. To measure similarity between multivoxel BOLD patterns during encoding and rest, we correlated each encoding matrix (high and low reward separately) with pre- and posttask rest matrices and Fisher z-transformed these correlation values to be used in group analyses. MVCS pattern similarity measures were calculated using custom Python (v3.11.11) scripts. Group analyses first used a LME to test for a Drug*Reward*Stage interaction predicting encoding–rest pattern similarity. We also used a separate LME to test for relationships between reinstatement (i.e., post- and pre-encoding rest pattern similarity) and item memory [hit rate − false alarm rate ~ reinstatement*reward*drug + age + sex + (1|subject)]. Finally, we tested for relationships between reinstatement and [^{11}C]raclopride [reinstatement ~ baseline [^{11}C]raclopride*drug*reward + age + sex + (1|subject)] and between [^{11}C]raclopride and change in reinstatement from placebo to drug [reinstatement (drug-placebo) ~ baseline [^{11}C]raclopride*drug + age + sex + (1|subject)].

RSFC Between the Hippocampus and SN/VTA. To investigate how connectivity between the hippocampus and SN/VTA changed from pretask to posttask and from placebo to drug, we used seed-to-seed RSFC. Time series (averaged across all voxels) were extracted using custom Python scripts for the hippocampus and SN/VTA ROIs from pretask and posttask preprocessed resting-state scans separately for placebo and drug and Fisher z-transformed Pearson correlations were computed. Drug*Stage LME interaction models tested for changes in RSFC from pretask to posttask on placebo and drug. Additionally, we tested for relationships between RSFC and item memory [hit rate − false alarm rate ~ RSFC (post-pre)*reward*drug + age + sex + (1|subject)] and between RSFC and [^{11}C]raclopride [RSFC (post-pre) ~ baseline [^{11}C]raclopride*drug + age + sex + (1|subject)].

[^{11}C]raclopride PET Acquisition and Processing. Thirty-one participants had baseline (placebo) [^{11}C]raclopride PET scans. Though we aimed to collect [^{11}C]raclopride PET scans during both placebo and drug sessions, tracer synthesis issues led to only 17 participants with usable scans for both placebo and drug sessions. We therefore focused our analyses on the larger sample of participants with at least a baseline (placebo) [^{11}C]raclopride scan. [^{11}C]raclopride binds D2/3 receptors competitively with endogenous dopamine and provides a measure of D2/3 receptor density (28, 39). The tracer was synthesized by the Radiochemistry Lab at the Martinos Center for Biomedical Imaging (Massachusetts General Hospital). Participants were injected with approximately 10 mCi of [^{11}C]raclopride as a bolus in an antecubital vein, and dynamic acquisition frames were obtained over 60 min in 3D mode: 5 × 1, 3 × 2, 3 × 3, 8 × 5 (19 frames total), as previously described (40). Images were corrected for attenuation using an MR-based statistical parametric mapping (SPM) pseudocomputed tomography method (61). PET data were further corrected for decay, random coincidences, detector sensitivity, and dead time (62). Frames were reconstructed using the three-dimensional ordinary Poisson ordered-subset expectation maximization (3D OP-OSEM) algorithm (62). Images were reconstructed in native space with 256 × 256 pixels, and 1 mm isotropic voxel size in units of becquerel/mL (bqml).

Preprocessing and data analysis were carried out using each participant's native space [^{11}C]raclopride scan. Standard preprocessing (realignment, coregistration) was performed using FSL. Reversible tracer binding was quantified using PMOD software (v4.0) to implement a simplified reference tissue model (SRTM) analysis with an occipital reference region (bilateral lingual and cuneus FreeSurfer ROIs). SRTM analysis was used to determine nondisplaceable binding potential (BP_{ND}), which can be defined by the equation $BP_{ND} = k_3/k_4$ where k_3 is the rate constant for the nondisplaceable tracer transfer between compartment and k_4 is the rate constant for the specifically bound tracer transfer between compartments (63). BP_{ND} values were extracted from the DCA separately for the left and right hemispheres using PMOD. A bilateral DCA ROI was created using weighted averages based on the number of voxels in each hemispheric ROI. We abbreviate [^{11}C]raclopride BP_{ND} as D2DR.

Pharmacological Protocol. Participants received an oral placebo and 20 mg oral methylphenidate during separate scans and were blind to drug condition. Safety procedures included a medical history and physical exam with a nurse practitioner, an electrocardiogram (EKG) performed before drug administration and before participant release at the end of the visit, and a urine drug screen. Consistent with previous research (40), the placebo was always administered for the first scan due to considerations surrounding methylphenidate metabolism. The placebo scan acted as a baseline measure of [^{11}C]raclopride binding. Methylphenidate was administered 45 min before the start of the second scan. Methylphenidate blocks dopamine reuptake into the presynaptic neuron by binding to dopamine transporters, thus increasing dopamine availability in the synapse (64).

Statistical Analyses. All statistical analyses were performed using R (v4.3.2). All interaction models were assessed with LME models with random intercepts and fixed slopes using the lme4 package (v1.1–35.5). All models included age and sex as covariates. Adding years of education and weight as additional covariates did not change results (*SI Appendix*, Tables S1–S3). Due to the limited sample size, we report only age and sex as covariates in our primary models. Effect sizes were reported as Cohen's partial f^2. As we are underpowered to detect three-way interactions (e.g., Drug*Reward*D2DR predicting pattern similarity and memory), we conducted parallel two-way Drug*D2DR analyses to confirm that our main findings do not change when we simplify the models. The results of these two-way models are reported in *SI Appendix*.

Data, Materials, and Software Availability. Human imaging and behavioral data have been deposited in Open Science Framework (https://doi.org/10.17605/OSF.IO/FCH8B) (65).

ACKNOWLEDGMENTS. This research was supported by the NIH National Institute on Aging (F31AG085963, F32AG084259, and R00AG058748).

Author affiliations: [a]Psychology Department, Brandeis University, Waltham, MA 02153; [b]Martinos Center for Biomedical Imaging, Massachusetts General Hospital, Boston, MA 02129; [c]Nathan Kline Institute for Psychiatric Research, Orangeburg, NY 10962; [d]Depression Clinical and Research Program, Massachusetts General Hospital, Boston, MA 02114; and [e]Life Sciences, Volen Center for Complex Systems, Brandeis University, Waltham, MA 02153

1. N. Karalija *et al.*, Longitudinal support for the correlative triad among aging, dopamine D2-like receptor loss, and memory decline. *Neurobiol. Aging* **136**, 125–132 (2024).
2. T. M. Karrer, A. K. Josef, R. Mata, E. D. Morris, G. R. Samanez-Larkin, Reduced dopamine receptors and transporters but not synthesis capacity in normal aging adults: A meta-analysis. *Neurobiol. Aging* **57**, 36–46 (2017).
3. L. Bäckman, L. Nyberg, U. Lindenberger, S.-C. Li, L. Farde, The correlative triad among aging, dopamine, and cognition: Current status and future prospects. *Neurosci. Biobehav. Rev.* **30**, 791–807 (2006).
4. J. Spaniol, C. Schain, H. J. Bowen, Reward-enhanced memory in younger and older adults. *J. Gerontol. B. Psychol. Sci. Soc. Sci.* **69**, 730–740 (2014).
5. A. Gasbarri, C. Verney, R. Innocenzi, E. Campana, C. Pacitti, Mesolimbic dopaminergic neurons innervating the hippocampal formation in the rat: A combined retrograde tracing and immunohistochemical study. *Brain Res.* **668**, 71–79 (1994).
6. S. Li, W. K. Cullen, R. Anwyl, M. J. Rowan, Dopamine-dependent facilitation of LTP induction in hippocampal CA1 by exposure to spatial novelty. *Nat. Neurosci.* **6**, 526–531 (2003).
7. C. G. McNamara, Á. Tejero-Cantero, S. Trouche, N. Campo-Urriza, D. Dupret, Dopaminergic neurons promote hippocampal reactivation and spatial memory persistence. *Nat. Neurosci.* **17**, 1658–1660 (2014).
8. K. C. Dickerson, R. A. Adcock, "Motivation and Memory" in *Stevens' Handbook of Experimental Psychology and Cognitive Neuroscience*, (John Wiley & Sons Ltd, 2018), pp. 1–36.
9. A. Patil, V. P. Murty, J. E. Dunsmoor, E. A. Phelps, L. Davachi, Reward retroactively enhances memory consolidation for related items. *Learn. Mem.* **24**, 65–69 (2017).
10. S.-H. Wang, R. G. M. Morris, Hippocampal-neocortical interactions in memory formation, consolidation, and reconsolidation. *Annu. Rev. Psychol.* **61**, C1–C4 (2010).
11. I. Bethus, D. Tse, R. G. M. Morris, Dopamine and memory: Modulation of the persistence of memory for novel hippocampal NMDA receptor-dependent paired associates. *J. Neurosci.* **30**, 1610–1618 (2010).

12. C. M. O'Carroll, S. J. Martin, J. Sandin, B. Frenguelli, R. G. M. Morris, Dopaminergic modulation of the persistence of one-trial hippocampus-dependent memory. *Learn. Mem.* **13**, 760–769 (2006).
13. J. I. Rossato, L. R. M. Bevilaqua, I. Izquierdo, J. H. Medina, M. Cammarota, Dopamine controls persistence of long-term memory storage. *Science* **325**, 1017–1020 (2009).
14. J. Lisman, A. A. Grace, E. Duzel, A neohebbian framework for episodic memory; Role of dopamine-dependent late LTP. *Trends Neurosci.* **34**, 536–547 (2011).
15. M. F. Carr, S. P. Jadhav, L. M. Frank, Hippocampal replay in the awake state: A potential substrate for memory consolidation and retrieval. *Nat. Neurosci.* **14**, 147–153 (2011).
16. J. O'Neill, B. Pleydell-Bouverie, D. Dupret, J. Csicsvari, Play it again: Reactivation of waking experience and memory. *Trends Neurosci.* **33**, 220–229 (2010).
17. A. Tambini, L. Davachi, Persistence of hippocampal multivoxel patterns into postencoding rest is related to memory. *Proc. Natl. Acad. Sci.* **110**, 19591–19596 (2013).
18. M. J. Gruber, M. Ritchey, S.-F. Wang, M. K. Doss, C. Ranganath, Post-learning hippocampal dynamics promote preferential retention of rewarding events. *Neuron* **89**, 1110–1120 (2016).
19. V. P. Murty, A. Tompary, R. A. Adcock, L. Davachi, Selectivity in postencoding connectivity with high-level visual cortex is associated with reward-motivated memory. *J. Neurosci.* **37**, 537–545 (2017).
20. A. Tambini, M. D'Esposito, Causal contribution of awake post-encoding processes to episodic memory consolidation. *Curr. Biol.* **30**, 3533–3543.e7 (2020).
21. R. Cools, M. D'Esposito, Inverted-U–shaped dopamine actions on human working memory and cognitive control. *Biol. Psychiatry* **69**, e113–e125 (2011).
22. R. Cools, T. W. Robbins, Chemistry of the adaptive mind. *Philos. Transact.: Math. Phys. Eng. Sci.* **362**, 2871–2888 (2004).
23. J. X. Cai, A. F. Arnsten, Dose-dependent effects of the dopamine D1 receptor agonists A77636 or SKF81297 on spatial working memory in aged monkeys. *J. Pharmacol. Exp. Ther.* **283**, 183–189 (1997).
24. A. G. Phillips, S. Ahn, S. B. Floresco, Magnitude of dopamine release in medial prefrontal cortex predicts accuracy of memory on a delayed response task. *J. Neurosci.* **24**, 547–553 (2004).
25. V. S. Mattay *et al.*, Catechol O-methyltransferase val158-met genotype and individual variation in the brain response to amphetamine. *Proc. Natl. Acad. Sci. U.S.A.* **100**, 6186–6191 (2003).
26. R. Cools *et al.*, Striatal dopamine predicts outcome-specific reversal learning and its sensitivity to dopaminergic drug administration. *J. Neurosci.* **29**, 1538–1543 (2009).
27. R. Kuczenski, D. S. Segal, Effects of methylphenidate on extracellular dopamine, serotonin, and norepinephrine: Comparison with amphetamine. *J. Neurochem.* **68**, 2032–2037 (1997).
28. N. D. Volkow *et al.*, Dopamine transporter occupancies in the human brain induced by therapeutic doses of oral methylphenidate. *Am. J. Psychiatry* **155**, 1325–1331 (1998).
29. E. J. Hermans *et al.*, Persistence of amygdala–hippocampal connectivity and multi-voxel correlation structures during awake rest after fear learning predicts long-term expression of fear. *Cereb. Cortex* **27**, 3028–3041 (2017).
30. A. M. Gordon, J. Rissman, R. Kiani, A. D. Wagner, Cortical reinstatement mediates the relationship between content-specific encoding activity and subsequent recollection decisions. *Cereb. Cortex* **24**, 3350–3364 (2014).
31. T. H. Wang, J. D. Johnson, M. de Chastelaine, B. E. Donley, M. D. Rugg, The effects of age on the neural correlates of recollection success, recollection-related cortical reinstatement, and post-retrieval monitoring. *Cereb. Cortex* **26**, 1698–1714 (2016).
32. J. Kukolja, D. Y. Göreci, Ö. A. Onur, V. Riedl, G. R. Fink, Resting-state fMRI evidence for early episodic memory consolidation: Effects of age. *Neurobiol. Aging* **45**, 197–211 (2016).
33. H. I. L. Jacobs *et al.*, Consolidation in older adults depends upon competition between resting-state networks. *Front. Aging Neurosci.* **6**, 344 (2015).
34. A. M. W. Linssen, E. F. P. M. Vuurman, A. Sambeth, W. J. Riedel, Methylphenidate produces selective enhancement of declarative memory consolidation in healthy volunteers. *Psychopharmacology* **221**, 611–619 (2012).
35. H. J. Bowen, J. H. Ford, C. L. Grady, J. Spaniol, Frontostriatal functional connectivity supports reward-enhanced memory in older adults. *Neurobiol. Aging* **90**, 1–12 (2020).
36. M. Mather, A. Schoeke, Positive outcomes enhance incidental learning for both younger and older adults. *Front. Neurosci.* **5**, 129 (2011).
37. L. Nyberg *et al.*, Dopamine D2 receptor availability is linked to hippocampal–caudate functional connectivity and episodic memory. *Proc. Natl. Acad. Sci.* **113**, 7918–7923 (2016).
38. G. Papenberg *et al.*, Mapping the landscape of human dopamine D2/3 receptors with [11C] raclopride. *Brain Struct. Funct.* **224**, 2871–2882 (2019).
39. C. J. Endres *et al.*, Kinetic modeling of [11C]raclopride: Combined PET–microdialysis studies. *J. Cereb. Blood Flow Metab.* **17**, 932–942 (1997).
40. A. S. Berry *et al.*, Dopamine synthesis capacity is associated with D2/3 receptor binding but not dopamine release. *Neuropsychopharmacol.* **43**, 1201–1211 (2018).
41. B. C. Wittmann *et al.*, Reward-related fMRI activation of dopaminergic midbrain is associated with enhanced hippocampus- dependent long-term memory formation. *Neuron* **45**, 459–467 (2005).
42. E. Aarts *et al.*, Dopamine and the cognitive downside of a promised bonus. *Psychol. Sci.* **25**, 1003–1009 (2014).
43. C. Davis *et al.*, Reward sensitivity and the D2 dopamine receptor gene: A case-control study of binge eating disorder. *Prog. Neuropsychopharmacol. Biol. Psychiatry* **32**, 620–628 (2008).
44. J. J. MacInnes, K. C. Dickerson, N. Chen, R. A. Adcock, Cognitive neurostimulation: Learning to volitionally sustain ventral tegmental area activation. *Neuron* **89**, 1331–1342 (2016).
45. A. H. Sinclair, Y. C. Wang, R. A. Adcock, Instructed motivational states bias reinforcement learning and memory formation. *Proc. Natl. Acad. Sci.* **120**, e2304881120 (2023).
46. J. D. Koen, M. D. Rugg, Neural dedifferentiation in the aging brain. *Trends Cogn. Sci.* **23**, 547–559 (2019).
47. L. Deng *et al.*, Age-related dedifferentiation and hyperdifferentiation of perceptual and mnemonic representations. *Neurobiol. Aging* **106**, 55–67 (2021).
48. H. Abdulrahman, P. C. Fletcher, E. Bullmore, A. M. Morcom, Dopamine and memory dedifferentiation in aging. *Neuroimage* **153**, 211–220 (2017).
49. P. Piolino *et al.*, Reduced specificity of autobiographical memory and aging: Do the executive and feature binding functions of working memory have a role?. *Neuropsychologia* **48**, 429–440 (2010).
50. B. R. King, M. A. Gann, D. Mantini, J. Doyon, G. Albouy, Persistence of hippocampal and striatal multivoxel patterns during awake rest after motor sequence learning. *iScience* **25**, 105498 (2022).
51. B. Tanrıverdi *et al.*, Awake hippocampal–cortical co–reactivation is associated with forgetting. *J. Cogn. Neurosci.* **35**, 1446–1462 (2023).
52. A. C. Schapiro, E. A. McDevitt, T. T. Rogers, S. C. Mednick, K. A. Norman, Human hippocampal replay during rest prioritizes weakly learned information and predicts memory performance. *Nat. Commun.* **9**, 3920 (2018).
53. J. R. Winer *et al.*, Sleep as a potential biomarker of tau and β-amyloid burden in the human brain. *J. Neurosci.* **39**, 6315–6324 (2019).
54. I. C. Ballard *et al.*, Temporal fMRI dynamics map dopamine physiology. bioXriv [Preprint] (2025), https://doi.org/10.1101/2025.03.24.645022 (Accessed 24 August 2025).
55. M. J. Dahl *et al.*, The integrity of dopaminergic and noradrenergic brain regions is associated with different aspects of late-life memory performance. *Nat. Aging* **3**, 1128–1143 (2023).
56. D. D. Garrett *et al.*, Amphetamine modulates brain signal variability and working memory in younger and older adults. *Proc. Natl. Acad. Sci.* **112**, 7593–7598 (2015).
57. C. Catana *et al.*, Toward implementing an MRI-based PET attenuation-correction method for neurologic studies on the MR-PET brain prototype. *J. Nucl. Med.* **51**, 1431–1438 (2010).
58. O. Mawlawi *et al.*, Imaging human mesolimbic dopamine transmission with positron emission tomography: I. Accuracy and precision of D_2 receptor parameter measurements in ventral striatum. *J. Cereb. Blood Flow Metab.* **21**, 1034–1057 (2001).
59. M. Reuter, B. Fischl, Avoiding asymmetry-induced bias in longitudinal image processing. *Neuroimage* **57**, 19–21 (2011).
60. V. P. Murty *et al.*, Resting state networks distinguish human ventral tegmental area from substantia nigra. *Neuroimage* **100**, 580–589 (2014).
61. D. Izquierdo-Garcia *et al.*, An SPM8-based approach for attenuation correction combining segmentation and nonrigid template formation: Application to simultaneous PET/MR brain imaging. *J. Nucl. Med.* **55**, 1825–1830 (2014).
62. D. B. Chonde, D. Izquierdo-Garcia, K. Chen, S. L. Bowen, C. Catana, Masamune: A tool for automatic dynamic PET data processing, image reconstruction and integrated PET/MRI data analysis. *EJNMMI Phys.* **1**, A57 (2014).
63. A. A. Lammertsma, S. P. Hume, Simplified reference tissue model for PET receptor studies. *Neuroimage* **4**, 153–158 (1996).
64. T. D. Challman, J. J. Lipsky, Methylphenidate: Its pharmacology and uses. *Mayo Clin. Proc.* **75**, 711–721 (2000).
65. C. Ciampa. "Dopaminergic mechanisms supporting hippocampal post-encoding dynamics in humans". Open Science Framework. https://dx.doi.org/10.17605/OSF.IO/FCH8B. Deposited 22 September 2025.